Neurochemical Research (2019) 44:2708–2722
https://doi.org/10.1007/s11064-019-02889-z

ORIGINAL PAPER

Icariin Ameliorates Amyloid Pathologies by Maintaining Homeostasis of Autophagic Systems in $A\beta_{1-42}$-Injected Rats

Xia Jiang[1,2] · Lin-Lin Chen[2] · Zhou Lan[2] · Fan Xiong[1] · Xiang Xu[1] · Yang-Yang Yin[1] · Ping Li[1] · Ping Wang[2]

Received: 30 March 2019 / Revised: 26 September 2019 / Accepted: 3 October 2019 / Published online: 15 October 2019

Abstract

Macroautophagy, a sole pathway for dysfunctional organelles or aggregated proteins turnover, has been implicated in the early development of Alzheimer's disease (AD). Previous studies have found that reversal of autophagy dysfunction in APP transgenic mice ameliorates amyloid pathologies. Icariin (ICA), the main component from traditional Chinese herb *Epimedium brevicornu* Maxim., can reduce accumulations of amyloid-β (Aβ) peptide in vivo and in vitro, but the mechanism remains unclear. Here, we explored the effects of ICA on autophagy-lysosomal pathway in intracerebroventricular (icv) injection of human $A\beta_{1-42}$ peptide rats. We demonstrated that feeding the rats with ICA (30 mg/kg, 60 mg/kg and 90 mg/kg rat, per os) for 4 weeks rescued the $A\beta_{1-42}$-induced spatial memory impairments, reduced endogenous rat $A\beta_{42}$ tested by ELISA and decreased Aβ accumulation using 6E10 antibody. Furthermore, $A\beta_{1-42}$ induced strong autophagy response, however ICA decreased the levels of microtubule-associated protein 1 light chain 3 (LC3) II/LC3I, Beclin1, Cathepsin D (Cat D) and brain lysosomal Cathepsin D activity. We also observed that ICA enhanced the phosphorylation of protein kinase B (PKB/AKT) and p70 ribosomal protein S6 kinase (p70S6K). In addition, ICA arrested $A\beta_{1-42}$-induced cells loss, mitochondrias damage, nuclear membranes unclear and abundant nucleas chromatin agglutinates in hippocampus, lessened the expression of Cleaved-caspase-3, brain oxidative stress, astroglial activation. These findings suggest that ICA can ameliorate amyloid pathologies with improving autophagy-lysosome function and Chinese materia medica may be potential for AD treatment.

Keywords Alzheimer's disease · Memory deficit · Autophagy · Aβ · Protein aggregation

Introduction

Alzheimer's disease (AD) is the most common cause of progressive impairment of cognitive functions in humans during aging. Amyloid-β (Aβ) peptide, a 4-kDa peptide derived from the sequential cleavage of amyloid precursor protein (APP) by β- and γ-secretase, which has been well characterized biochemically [1–3]. Aβ accumulation in the form of extracellular senile plaques (SPs) abnormally in the brain are considered to trigger the AD pathogenesis [2, 3]. Neuronal expression of mutants of APP in animal models results in Aβ deposition, gliosis, and impaired cognitive functions [4]. Clinically, the number of argyrophilic plaques is not closely correlated with severity of AD [5–8]. Strikingly, memory impairments can occur in the absence of Aβ plaque in APP overexpression models, and intracellular Aβ peptides may cause the cognitive deficits [7, 9]. Valuable findings emphasize that oligomeric forms of Aβ peptides, increasing in ageing and AD located in pyramidal neurons of the hippocampus and layer II of entorhinal cortex, is thought to be neurotoxic and to impair learning and memory, synaptic plasticity and hippocampal long-term potentiation (LTP) [10–12]. These evidences support that Aβ is toxic intracellularly before it is released to form Aβ deposits extracellularly. $A\beta_{42}$ has a greater propensity to selfaggregate into insoluble fibrils and more neurotoxicity than $A\beta_{40}$ [13]. Aβ oligomers

Electronic supplementary material The online version of this article (https://doi.org/10.1007/s11064-019-02889-z) contains supplementary material, which is available to authorized users.

✉ Xia Jiang
jane_j_09@126.com

✉ Ping Wang
pwang54@aliyun.com

[1] Department of Pathology, Hubei University of Chinese Medicine, Wuhan 430065, People's Republic of China

[2] New products of TCM senile Diseases Co-innovation Center of Hubei, Wuhan 430065, People's Republic of China

(AβOs) now widely regarded as instigating neuron damage leading to Alzheimer's dementia [14, 15]. It has been found that human $A\beta_{1-42}$ peptide intracerebroventricular infusion induced impaired learning and memory and neuronal dysfunction without Aβ deposits [16, 17], widely used as a non-transgenic animal model for AD.

Most neurodegenerative diseases are characterized by the accumulation of misfolded proteins [18]. Macroautophagy (hereafter referred to as autophagy) is an evolutionarily conserved process, which is a pathway for long-lived protein and cytoplasmic organelles by lysosomal enzymes [19–21]. Autophagy is highly dynamic and involves multiple steps, including initial formation of double membranes, maturation of autophagosomes through fusion with lysosomes, then formation of autolysosomes for degradation [22]. Aβ generated in endosomes and autophagic vacuoles, then delivered to lysosomes and cleared through lysosomal proteolysis under normal conditions [23]. However, the maturation of autophagolysosomes and their retrograde transport may be impaired in AD patients and transgenic AD mice, which leads to a large number of Aβ-containing autophagic vacuoles markedly accumulated in dystrophic neurites before extracellular Aβ deposition [24, 25]. Particularly, it has been demonstrated that suppression of basal autophagy leads to elevated Aβ accumulation aggregation and causes neurodegeneration [26, 27]. Conversely, increasing autophagy is predicted to be beneficial for reducing accumulations of Aβ peptide and ubiquitinated proteins [28, 29]. Therefore, modulation of autophagy dysfunction is a fundamental strategy that may intervene the pathology of AD.

Icariin (ICA) the main component from traditional Chinese herb *Epimedium brevicornu* Maxim., which exerts osteogenic differentiation, antitumor, and estrogen-like pharmacological activities [30–33]. ICA can rescue major AD hallmarks in AD, including (i) that it improved learning and memory abilities in aged rats, $A\beta_{25-35}$ hippocampal injected rats, senescence-accelerated mouse prone 8 (SAMP8) mice and transgenic AD mice [34–37]; (ii) that it attenuated Aβ-induced neurotoxicity by inhibition of tau protein hyperphosphorylation in cultured rat pheochromocytoma PC12 cells [38]; (iii) that it attenuated synaptic and cognitive deficits by $A\beta_{1-42}$ in vivo [39]; (iv) that it reduced the Aβ burden and plaque deposition by decreasing the APP and β-Site APP-cleaving enzyme 1 (BACE1) in APP transgenic mice [40]. Recently, it was shown that ICA possesses anti-inflammation and antioxidation neuroprotective effects [41, 42], suggesting that it maybe a scavenger for both reactive oxygen species (ROS) and Aβ. Here, we injected human $A\beta_{1-42}$ peptide into the intracerebroventricular (icv) of male Sprague–Dawley (SD) rats and feeded the rats with ICA to examine the effects of ICA on autophagic process in vivo.

Materials and Methods

Antibodies and Chemicals

ICA ($C_{33}H_{40}O_{15}$, molecular weight: 676.67) was purchased from the National Institute for Food and Drug Control (Beijing, China). Powder of ICA (with 99% purity as determined by a high-performance liquid chromatography assay) was dissolved in absolute ethyl alcohol (final concentration no more than thousandth) and diluted in drinking water for 4 weeks. Human $A\beta_{1-42}$ peptide (Catalog: A9810), superoxide dismutase (SOD) determination kit (Catalog: 19160) and other chemicals were purchased from Sigma-Aldrich Chemical Co. (St Louis, MO, USA). DAB Detection Kit was from ZSGB Bio. Co. (Beijing, China). Bicinchoninic acid (BCA) kit, peroxidase-conjugated goat anti-rabbit and goat anti-mouse secondary antibodies were from Pierce (Rockford, IL, USA). The primary antibodies used in the experiments are listed in Table 1.

Animals and Treatments

Adult male SD rats (3–4 months old, 250 ± 50 g) were obtained from Hubei Province Academy of Preventive Medicine. Rats were group housed (4–5/cage) with ad libitum food and water and maintained on a reverse 12:12 light–dark cycle with lights on at 08:00 am at 20–22 °C room temperature. All procedures were conducted in accordance with the "Policies on the Use of Animals and Humans in Neuroscience Research" revised and approved by the Society for Neuroscience in 1995.

Human $A\beta_{1-42}$ peptide were oligomerized according to the procedure described previously [43]. In brief, $A\beta_{1-42}$ was dissolved in dimethyl sulfoxide (DMSO) and diluted in sterile physiological saline to a final concentration of 2.6 μg/μl. Then the solution was incubated at 37 °C in dark for 1 week for oligomerization before use. Since reverse amyloid protein 42-1 ($A\beta_{42-1}$) has no effects on learning ability and pathological changes in previous reports and our preliminary experiments, sterile physiological saline rather than $A\beta_{42-1}$ was used as control. The rats were randomly divided into five experimental groups (n = 10). The animals were anesthetized by chloral hydrate (36 mg/kg, i.p.) and placed on a stereotaxic instrument (Narishige Scientific Instrument Lab., Tokyo, Japan). The coordinates for the injection are AP-0.9 mm, L-1.5 mm and V-4 mm (from bregma and dura, flat skull) according to the stereotaxic atlas. 5 μl of the solution with $A\beta_{1-42}$ was infused into the lateral ventricle. After each injection, injectors were let in place for 10 min in order to avoid flow back of solution. The rats were fed orally with ICA (30 mg/day, 60 mg/day

Table 1 Antibodies used in this article

Antibody (type)	Specificity	Catalog	Source
APP (P)	Level of APP	07-667	Millipore Corporation (Billerica, MA, USA)
LC3 (P)	N-terminal portion of human microtubule-associated protein light chain 3	NB100-2220	Novus Biologicals (Littleton, Colorado, USA)
Beclin 1(M) for WB	Human beclin 1 171–291	612112	BD Biosciences (San Jose, CA)
Beclin 1(P) for IHC	Beclin 1 fusion protein Ag1843	11306-1-AP	Proteintech (Chicago, IL, USA)
Cat D (P)	Human cathepsin D	sc-10725	Santa Cruz (Santa Cruz, CA, USA)
P62 (P)	p62/SQSTM1	ab56416	Abcam (Cambridge, MA, USA)
Cleaved-caspase-3(P)	Cleaved Caspase-3 (Asp175)	#9661	Cell Signaling Technology Inc. (Beverly, MA, USA)
22C11 (M)	Amino acids 66–81 of N-terminus of APP	MAB348	Millipore Corporation (Billerica, MA, USA)
AKT (P)	Total AKT	#9272	Cell Signaling Technology Inc. (Beverly, MA, USA)
pS473AKT (P)	Phosphor-AKT at Serine 473	#9271	Cell Signaling Technology Inc. (Beverly, MA, USA)
p-p70S6K (M)	Phospho-p70 S6 Kinase (Thr389)	#9234	Cell Signaling Technology Inc. (Beverly, MA, USA)
p70S6K (P)	Total p70 S6 kinase protein	#9202	Cell Signaling Technology Inc. (Beverly, MA, USA)
Human $A\beta_{1-42}$ (P)	$A\beta_{1-42}$	bs-0107R	Bioss Inc. (Woburn, MA, USA)
6E10 (M)	$A\beta_{1-16}$	803014	BioLegend (San Diego, CA, USA)
GFAP (M)	Glial fibrillary acidic protein	60190-1-Ig	Proteintech (Chicago, IL, USA)
GAPDH (P)	GAPDH	AB2302	Millipore Corporation (Billerica, MA, USA)

M monoclonal antibody, *P* polyclonal antibody, *WB* western blotting, *IHC* immunohistochemistry

and 90 mg/day, the dose and duration were chosen referring to previous studies) before or after the icv injection.

Morris Water Maze (MWM)

The water maze (180-cm diameter, 60-cm high) was filled with water around 23 °C and made opaque by addition of a nontoxic black paint. Animals were trained to find a hidden platform (2 cm below the surface of the water in a fixed location in third quadrants) for 5 consecutive days and 4 trials per day with a 30 min interval. The releasing point was randomly distributed across four quadrants of the pool. For the probe trial, spatial memory retention of the rats was measured 24 h after the 5-days training by MWM test. Then the rats were anesthetized and decapitated and the hippocampi extracts or brain slices were prepared for further studies.

Western Blotting

Hippocampus homogenate and protein extraction was performed according to the procedure described previously [44]. The protein concentration was estimated by BCA kit according to manufacturer's instructions. The proteins were separated by 10% sodium dodecyl sulfate–polyacrylamide gel electrophoresis and transferred to polyvinylidene fluoride membrane. The membranes were probed with the following antibodies: APP, 22C11, LC3, Beclin1, Cat D, P62, total AKT, pS473AKT, p-p70S6K, p70S6K and GAPDH (all 1:1000 dilution) for overnight at 4 °C, then incubated with anti-mouse or anti-rabbit IgG conjugated to horseradish peroxidase (1:5000) for 1 h at 37 °C. The protein bands were visualized using the enhanced chemiluminescence (ECL) method and quantitatively analyzed by Kodak Digital Science 1D software (Eastman Kodak Company, New Haven, CT, USA).

For AβOs Western blotting, 10 μg samples were run on Tricine–SDS-PAGE gel electrophoresis, and transferred to nitrocellulose membrane and probed with human $A\beta_{1-42}$ (Bioss, Woburn, MA, USA). Then the blots were incubated with anti-rabbit IgG conjugated to IRDye (800 CW, Lincoln, NE, USA) for 1 h at room temperature and visualized using the Odyssey Infrared Imaging System (Lincoln, NE, USA).

Immunohistochemistry and Nissl Staining

Immunohistochemistry was performed according to the procedure described previously [45]. In brief, the 25 μm vibratome sections (Leica, VT1000S, Germany) were permeabilized with 0.3% H_2O_2–phosphate-buffered saline–1% Triton X-100 for 20 min to block endogenous peroxidase and blocked with 3% bovine serum albumin for 30 min and incubated with Cleaved-caspase-3, 6E10, Beclin 1 and GFAP (diluted 1:200) for 48 h at 4 °C. Immunoreaction was detected using horseradish peroxidase-labeled antibodies and visualized with the DAB Detection Kit (Olympus Optical, Japan).

Nissl Staining Solution (Cresyl Violet, Catalog: G1430) was from Beijing Solarbio Science & Technology Co., Ltd. (Beijing, China). Stained samples were then dehydrated rapidly with 95% alcohol, cleared with xylene and mounted

with the neutral resin. The intensity of images was quantitatively analyzed by Image Pro Plus 4.5 (Media Cybernetics Inc. Silver Spring, MD, USA). For each experimental group, we measured nine blinded slides (three arbitrary slides per rat). Mean density values were counted to estimate the intensity of immunohistochemical reaction.

ELISA

Hippocampus were homogenized in Tris Buffered Saline (50 mM Tris–HCl, pH 7.6, 150 mM NaCl) containing protease inhibitor. The homogenized mixes were briefly sonicated to sheer the DNA and centrifuged samples for 20 min at 1000×*g* according to the manufacturer's instructions. Remove particulates and lysates of brain tissue in aliquot at − 20 °C or − 80 °C for use. Concentrations of $A\beta_{42}$ were measured by a sandwich ELISA kit using a rat anti-$A\beta_{42}$ (Catalog: R1402) antibody, according to the manufacturer's instructions (Elabscience Biotechnology Co. Ltd., Hubei, China).

Enzymatic Activity Assays

Cathepsin D Activity Fluorometric Assay Kit (Catalog: K143) was from BioVision (BioVision, Inc., CA, USA) and performed according to the procedure.

Measurement of Malondialdehyde (MDA) and SOD

Homogenized brain tissue extracted with PBS was mixed with 1% phosphoric acid and 0.67% thiobarbituric acid for 1 h at 95 °C. The absorbance was measured at 532 nm. The MDA content was expressed in micromoles per mg protein. SOD content was determined with an SOD determination kit.

Measurement of the Brain Content of ICA

The rats were fed orally with ICA (30, 60 and 90 mg/day) for 4 weeks after $A\beta_{1–42}$ injection, then decapitated at the final day of 4 week-treatments and 1 week after 4 week-treatments. The concentration of ICA was determined in hippocampi of rats exposed to ICA by LC-MS/MS according to a reported method with some modification [46].

Golgi Staining and Dendritic Spine Density Analysis

Golgi staining was performed according to the procedure detailed previously. The images were observed under light microscope (SF100, Nikon, Tokyo, Japan). For analysis of dendritic spine density, the calculation always started from the same position at 50 to 75 μm from the soma in apical dendrites [47]. We carried out morphometry in 10 neurons per animal in each group (n = 3).

Transmission Electron Microscopy (TEM) and Ultrastructural Analyses

Vibratome brain sections were cut and post-fixed in 1% osmium tetroxide. Following alcohol dehydration, sections were embedded in EPON resin (EMS) and ultrathin sections prepared (EM UC7, Leica, Germany) and stained with uranyl acetate and lead citrate. Material was viewed by TEM (Tecnai G^2 20 TWIN, FEI, USA) at 200 kV and images were recorded. For each group, we measured 27 neurons in Hippocampus (at least nine neurons were analyzed per rat).

Statistical Analysis

Data were expressed as mean ± SD and analyzed using SPSS 10.0 statistical software (SPSS Inc., Chicago, IL, USA). When two groups were being compared, the significance of data was assessed by the 2-tailed Student unpaired t test. For comparison of multiple groups, 2-way analysis of variance (ANOVA), repeated-measures 2-way ANOVA, and 1-way ANOVA with Bonferroni's post hoc comparisons test was used. We also normalized the data and present them as relative values for better understanding in our art works.

Results

ICA Improves Cognitive Deficits and Reduces Aβ in $A\beta_{1–42}$ icv Injected Rats

Firstly, we confirmed the quality of oligomerization of $A\beta_{1–42}$ at 37 °C in dark for 1 week (Fig. 1b), then detected the effect of ICA on spatial memory retention in $A\beta_{1–42}$ icv injected rats. On the 1st day after icv injection surgery, the rats were fed orally with or without ICA for 4 weeks. Then,rats were trained on the MWM procedure for 5 consecutive days to remember the invisible hidden platform. The timeline of the experiments is described as Fig. 1a. The mean latencies of 4 trials in 5-days training session for 5 groups are shown in Fig. 1d. As expected, the time to find the hidden platform were remarkably prolonged in $A\beta_{1–42}$ icv injected rats as previously described and treatment with ICA mitigated the $A\beta_{1–42}$-induced delayed escape latencies (Fig. 1d), suggesting that spatial learning performance was improved by ICA in $A\beta_{1–42}$ icv injected rats. After the 5-days training and ensuring visual and physical skills were intact (Fig. 1e), platform was removed and spatial memory was tested in probe trials. We calculated the time spent in the target quadrant zone during the 60 s test. $A\beta_{1–42}$ icv injected rats failure to prefer the goal quadrant, however, ICA improved $A\beta_{1–42}$-induced spatial

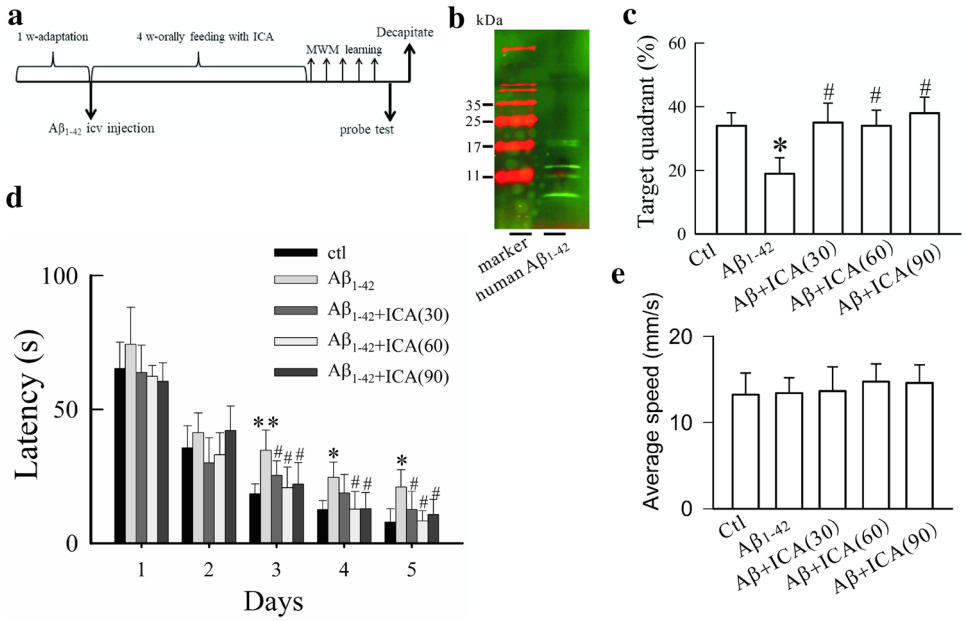

Fig. 1 ICA improves cognitive deficits in $A\beta_{1-42}$ icv injected rats. **a** A schematic diagram for the treatment of the rats; **b** to confirm the quality of oligomerization of Aβ, 10 μg sample was separated by tricine-SDS-PAGE gel electrophoresis using anti-human $A\beta_{1-42}$; **c** ICA increased percentage of residence time in target quadrant by probe test; **d** behavioral tests and quantitative analyses in the ICA cure experiment. The mean latencies (4 trials performances per day) were recorded for 5 consecutive days after ICA treatment for 4 weeks; **e** average speed of swimming in MWM (n = 10 rats each group) (Data were expressed as mean ± SD. Ctl, control group; $A\beta_{1-42}$, $A\beta_{1-42}$ icv injected rats; $A\beta_{1-42}$ + ICA(30), $A\beta_{1-42}$ + ICA(60) and $A\beta_{1-42}$ + ICA(90), ICA (30 mg/day, 60 mg/day and 90 mg/day respectively) $^{*}p < 0.05$; $^{**}p < 0.01$ vs Ctl (control group); $^{\#}p < 0.05$; $^{\#\#}p < 0.01$ vs $A\beta_{1-42}$ ($A\beta_{1-42}$ icv-injected group)

memory retention damage with more percentage of residence time in target quadrant (Fig. 1c).

Homogenates from the hippocampus were prepared and quantitative analysis of Western blotting using anti-APP and anti-22C11, which detect level of APP and amino acids 66–81 of N-terminus of APP respectively. Compared with the control rats, APP and 22C11 were significantly alleviated in the brains of $A\beta_{1-42}$ icv injected rats, however, ICA decreased levels of APP and ICA (at doses of 90 mg/day) decreased 22C11 (Fig. 2a). ELISA tests showed that ICA declined the levels of $A\beta_{42}$ in TBS fractions of hippocampal homogenates compared with model group (Fig. 2b).

In order to visualized Aβ distribution, a standard immunohistochemical procedure was processed using specific antibody 6E10 (against amino acids 1–16 of the Aβ peptide). There was almost no obvious intracellular staining to 6E10 in control group. Whereas the 6E10 positive staining was observed in cytoplasm of cortical and hippocampal neurons 5 weeks after $A\beta_{1-42}$ icv infusion, which was inhibited by ICA (60 mg/day) (Fig. 2c, d).

ICA Reverses Autophagic-Lysosomal Dysfunction Induced by $A\beta_{1-42}$

In the AD brains and in APPswe/PS1dE9 mice (overexpress mutant human PS1 and APP), accumulation of Aβ-containing autophagic vacuoles are observed in dystrophic neurites, which may be a site for Aβ production. Based on these findings, we next investigated ICA on autophagic process in $A\beta_{1-42}$ icv injected rats using the following antibodies to test the autophagic flux. Microtubule-associated protein 1 light chain 3-I (LC3-I), a cytosolic soluble protein, is converted to LC3-II that first appears on newly formed autophagosome and degraded quickly by lysosomal enzymes after autophagosome/lysosome fusion [48]. We observed the effects of ICA on the autophagy-related signaling by its acute and chronic treatments. The rats were received a single gavage of dissolved ICA (90 mg/kg) after $A\beta_{1-42}$ peptide injection and decapitated 24 h after gastrointestinal treatments. The hippocampi extracts were prepared for measuring the conversion of LC3-I into LC3-II to investigate autophagosome formation. Immunoblot analysis showed that high proportions of LC3-II/LC3-I in the hippocampus of $A\beta_{1-42}$ icv injected rats, indicating that Aβ activated the autophagic process, which consistent with previous results in vitro [49]. There were no significant differences of LC3-II/LC3-I between acute ICA treatments and $A\beta_{1-42}$ icv injected groups (Fig. S1). In contrast, compared to the model group, the levels of LC3-II/LC3-I were much lower in 4 week ICA administration groups and there were no detectable differences between ICA administration group and control group

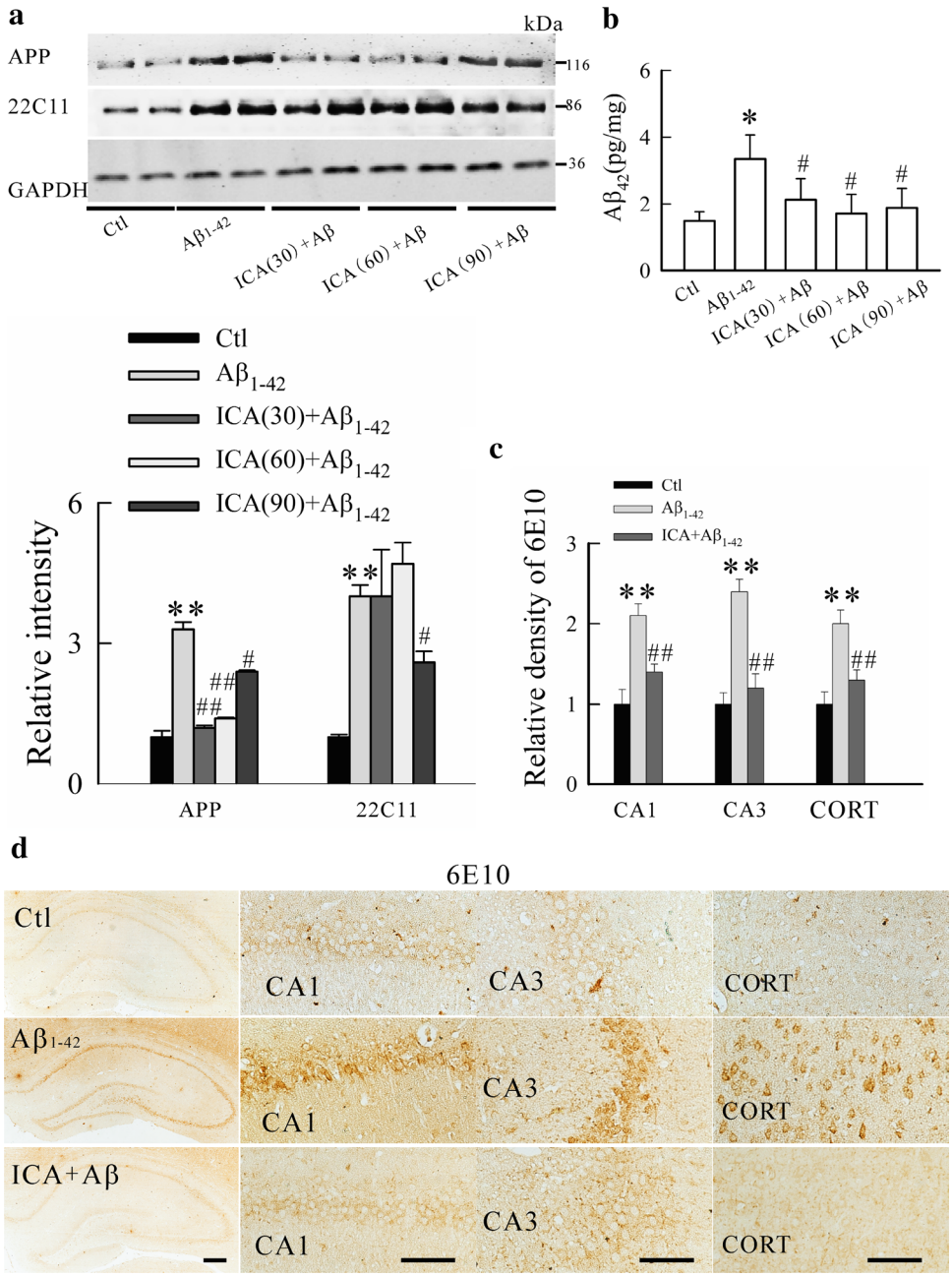

Fig. 2 Effects of ICA on APP processing and Aβ accumulation. **a** Western blotting and quantitative analysis for APP and 22C11 from the hippocampus; **b** the levels of $A\beta_{42}$ from hippocampal homogenates tested by ELISA; **c**, **d** immunohistochemical procedure was processed using specific antibody 6E10. Scale bars: 10 μm (Data were expressed as mean ± SD. Ctl, control group; $A\beta_{1-42}$, $A\beta_{1-42}$ icv injected rats; ICA(30) + $A\beta_{1-42}$, ICA(60) + $A\beta_{1-42}$ and ICA(90) + $A\beta_{1-42}$, ICA (30 mg/day, 60 mg/day and 90 mg/day respectively); CORT, cortex; $^{*}p < 0.05$; $^{**}p < 0.01$ vs Ctl (control group); $^{\#}p < 0.05$; $^{\#\#}p < 0.01$ vs $A\beta_{1-42}$ ($A\beta_{1-42}$ icv-injected group)

(Fig. 2a, b). These results means that chronic instead of acute ICA treatments can efficiently increase autolysosome turnover of LC3-II. To assess recruitment of membranes to form autophagosomes and protein degradation/clearance, we detected the key proteins using Beclin1 [50] and Cat D antibodies respectively by western blotting. Beclin1 and Cat D were strongly increased in the hippocampus of $A\beta_{1-42}$ icv injected animals, however, chronic ICA treatments obviously reduced the proteins compared with those in this AD model rats. It was interesting that there were no significantly differences in P62 levels between control and model groups (Fig. 3a, b). Then, we detected enzymatic activities of Cathepsin D in hippocampal homogenates. Enzymatic activities of Cathepsin D were higher in $A\beta_{1-42}$ icv injected rats brains than in control brains, however chronic ICA treatments decreased Cathepsin D activity (Fig. 3c).

Phosphorylation of the kinases mammalian target of rapamycin (mTOR) and p70S6K which modulate cell growth, proliferation and autophagy. Expression of p70S6K was examined using antibodies against its total and phosphorylated at Thr389 forms. In $A\beta_{1-42}$ icv injected rats homogenates, a decreased level of phosphorylated p70S6K was observed, however, a significant increase of p-p70S6K/

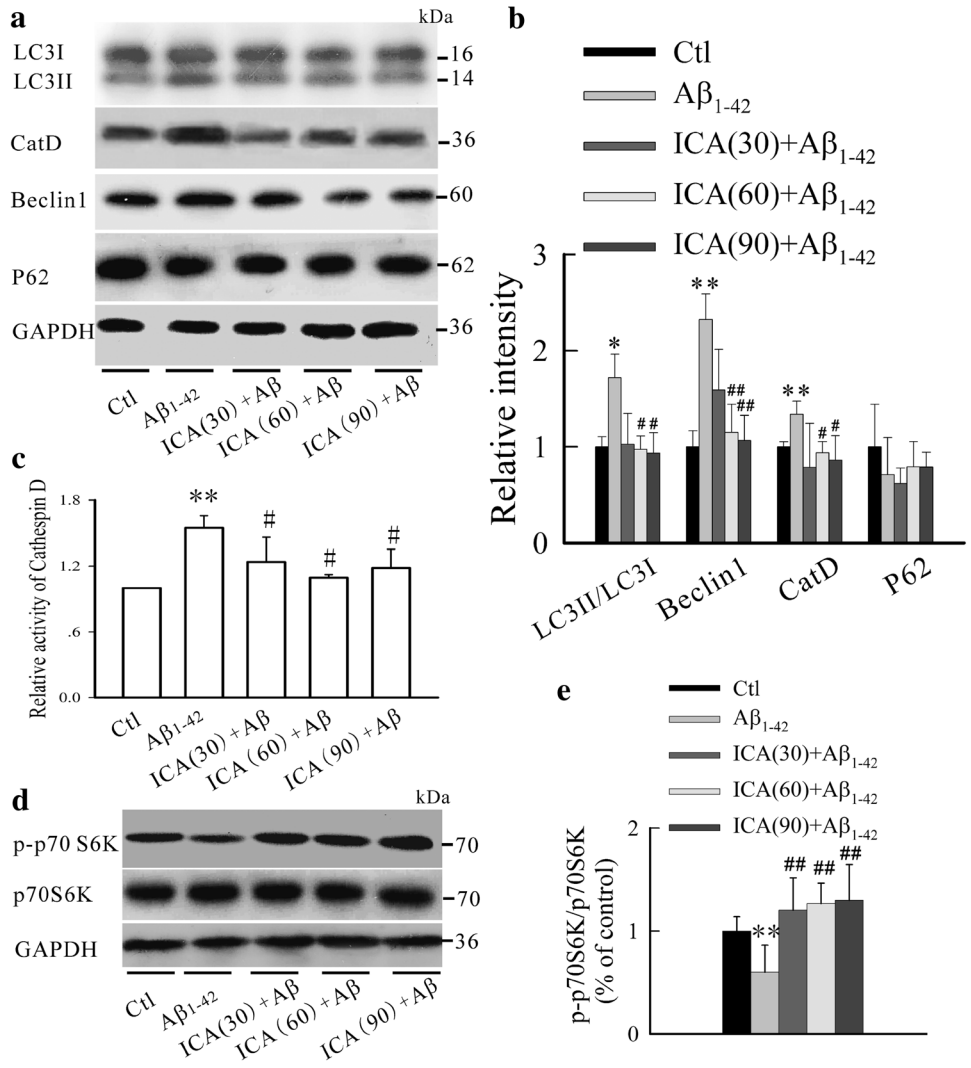

Fig. 3 ICA decreases $A\beta_{1-42}$-induced autophagic process activation in vivo. Animals were sacrificed and homogenates from the hippocampus were prepared 1 day after testing session. **a**, **b** Western blotting and quantitative analysis found that ICA decreased conversion of LC3-I into LC3-II, Beclin 1 and Cat D levels, which were increased in $A\beta_{1-42}$ icv injected rats normalized to GAPDH. There were no significantly difference in P62 levels normalized with respect to GAPDH; **c** enzymatic activities of Cathepsin D were higher in $A\beta_{1-42}$ icv injected rats brains than in control brains, however ICA decreased Cathepsin D activity; **d** p-p70S6K and total p70S6K were detected by Western blotting; **e** quantitative analysis of p-p70S6K/p70S6K. Data were expressed as mean ± SD, $^{*}p < 0.05$; $^{**}p < 0.01$ vs Ctl (control group); $^{\#}p < 0.05$; $^{\#\#}p < 0.01$ vs $A\beta_{1-42}$ ($A\beta_{1-42}$ icv-injected group)

p70S6K was analyzed in chronic ICA treatment groups (Fig. 3d, e).

The Beclin1-positive neurons were distributed in the CA1, CA3 and dentate gyrus (DG) regions of the hippocampus 5 weeks after $A\beta_{1-42}$ icv injection, whereas chronic ICA group revealed a decrease in the expression of Beclin1 detected by immunohistochemical analysis (Fig. 4a, b). At the ultrastructural level, there were active lysosome with digestion vacuoles in cytoplasm (Fig. 4c) and axon in hippocampal neurons of $A\beta_{1-42}$ icv injected rats (Fig. 4d) using Tecnai G^2 20 TEM. Dystrophic neurites are grossly enlarged containing predominantly AVs of varying morphologies in hippocampal neurons from $A\beta_{1-42}$ icv-injected rats (Fig. 4e) compared with neurites from control (Fig. 4f) and ICA rats (Fig. 4g). To explore the antioxidant system, MDA levels and SOD contents were measured. As expected, ICA treatment suppressed $A\beta_{1-42}$-triggered the levels of MAD (Fig. 4h), as well as SOD contents of the ICA group were higher than that of the model group (Fig. 4i).

Next, we measured the brain content of ICA at final day of 4 week-treatments and 1 week after 4 week-treatments to investigate whether ICA can penetrate the blood–brain barrier and the persistence of ICA's efficacy. Under the optimized LC-MS conditions, ICA was found with extremely low distribution in brain, which indicated that ICA could not efficiently cross the blood–brain barrier. Meanwhile, there were no significant differences between the two time points, demonstrating that the concentration of ICA did not decrease after 1 week of withdrawal and ICA in the brain may not regulate autophagy signals directly (Fig. S2).

Furthermore, to explore whether ICA canceled or offsetted the effect of Aβ, the rats were fed with ICA (30, 60 and 90 mg/kg) alone for 4 weeks. We didn't find that ICA could decrease endogenous rat $A\beta_{42}$ tested by ELISA (Fig. S3A), There were no significant changes of MAD and SOD (Fig. S3B, C), indicating that these doses of ICA hadn't neurotoxicity. These results suggesting that ICA maybe have a compensatory effects of reducing Aβ and neutralizing

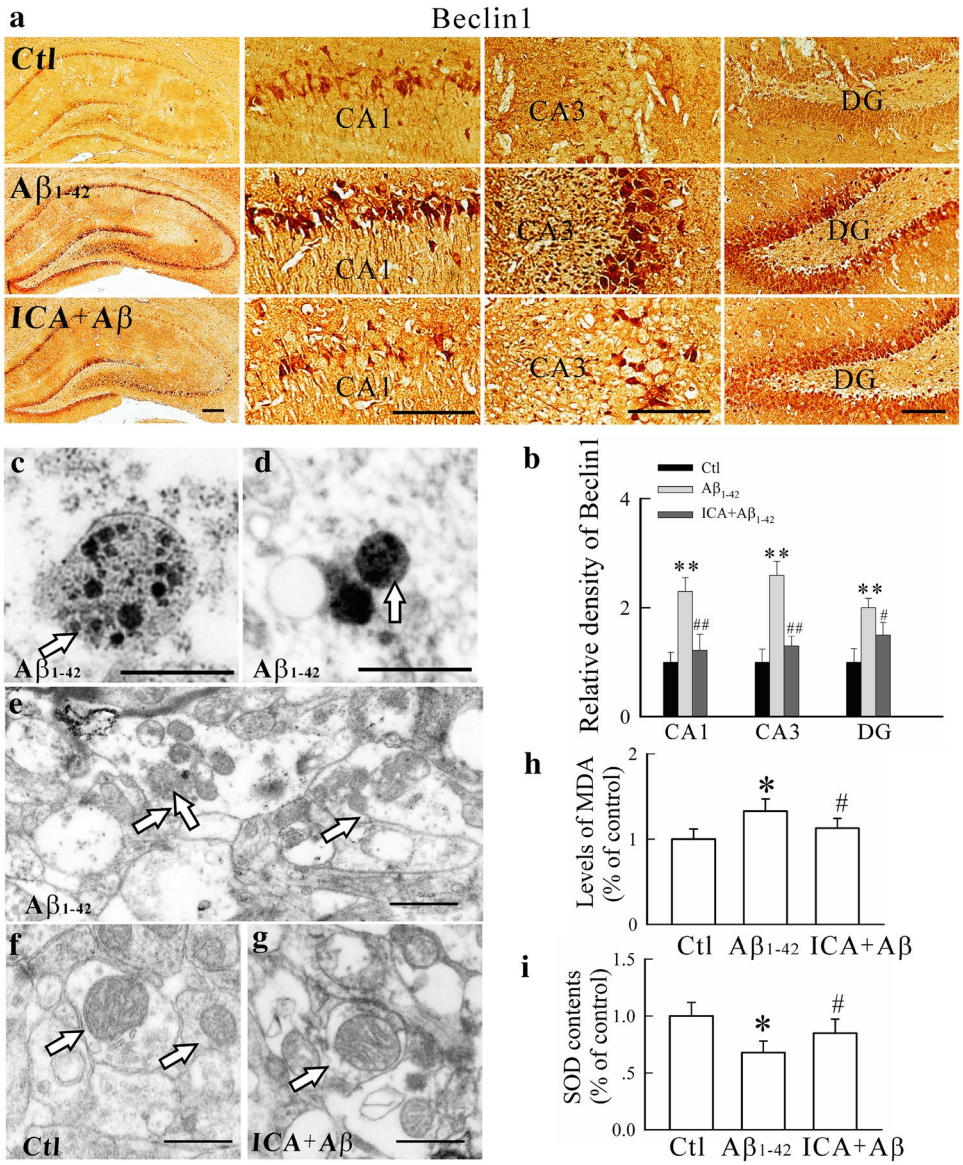

Fig. 4 ICA reduced Beclin1 expression and ameliorated dystrophic neurites and oxidative stress. **a**, **b** ICA reduced Beclin1-positive neurons distributed in hippocampus 5 weeks after $A\beta_{1–42}$ icv injection; Scale bars: 10 μm; Active lysosome with digestion vacuoles in cytoplasm (**c**) and axon (**d**) in $A\beta_{1–42}$ icv-injected rats by TEM. **e** Dystrophic neurites (arrows) contain predominantly AVs of varying morphologies in hippocampal neurons from $A\beta_{1–42}$ rats. By contrast, AVs are rare in control (**f**) and ICA brain (**g**); **h**, **i** ICA had antioxidation to antagonize $A\beta_{1–42}$. Scale bars: 500 nm. Data were expressed as mean ± SD (n = 3 rats each group). *p < 0.05; **p < 0.01 vs Ctl (control group); #p < 0.05; ##p < 0.01 vs $A\beta_{1–42}$ ($A\beta_{1–42}$ icv-injected group)

the toxicity of Aβ in vivo. The ratios of LC3-II/LC3-I in ICA (90 mg/kg) group were much higher than that in other groups, however, Beclin1 and Cat D had not changes in four groups (Fig. S3D, E).

ICA Reduces Cleaved-Caspase-3 Expression, Astroglial Reaction and Rescues Ultrastructure in Hippocampus of $A\beta_{1–42}$ icv Injected Rats

It has been known that Aβ peptide induces apoptotic cell death through mitochondrial toxicity and caspase-3 activation [51–54]. Therefore, we evaluated the effects of ICA on expression of Cleaved-caspase-3 protein and ultrastructure of hippocampal neurons. Quantitative analysis showed that ICA (60 mg/day) attenuated the $A\beta_{1–42}$-induced increase of Cleaved-caspase-3 levels in hippocampus (Fig. 5a, b). In the CA1 and CA3 regions of the hippocampus, $A\beta_{1–42}$ injection significantly induced a decrease in the number of pyramidal cells, while ICA inhibited cell loss using Nissl staining (Fig. 6c, d). To understand whether upstream molecule protein kinase B (PKB/AKT) were involved in anti-apoptosis effect of ICA, we measured the activity-dependent phosphorylation level of AKT at serine 473 (pS473AKT). We found that ICA obviously increased the ratio of pS473AKT/AKT (Fig. 5c, d).

Next, we performed studies on ultrastructure of mitochondrias and nuclei in the brains. Electron micrographs of the CA1 hippocampal area showed that control rats had normal mitochondrias with two bounding membranes enriched in regions of active synapses and nuclei possess clear membranes. $A\beta_{1–42}$ icv injected rats had damage mitochondrias reflected by the degree of the swelling in dystrophic neurites

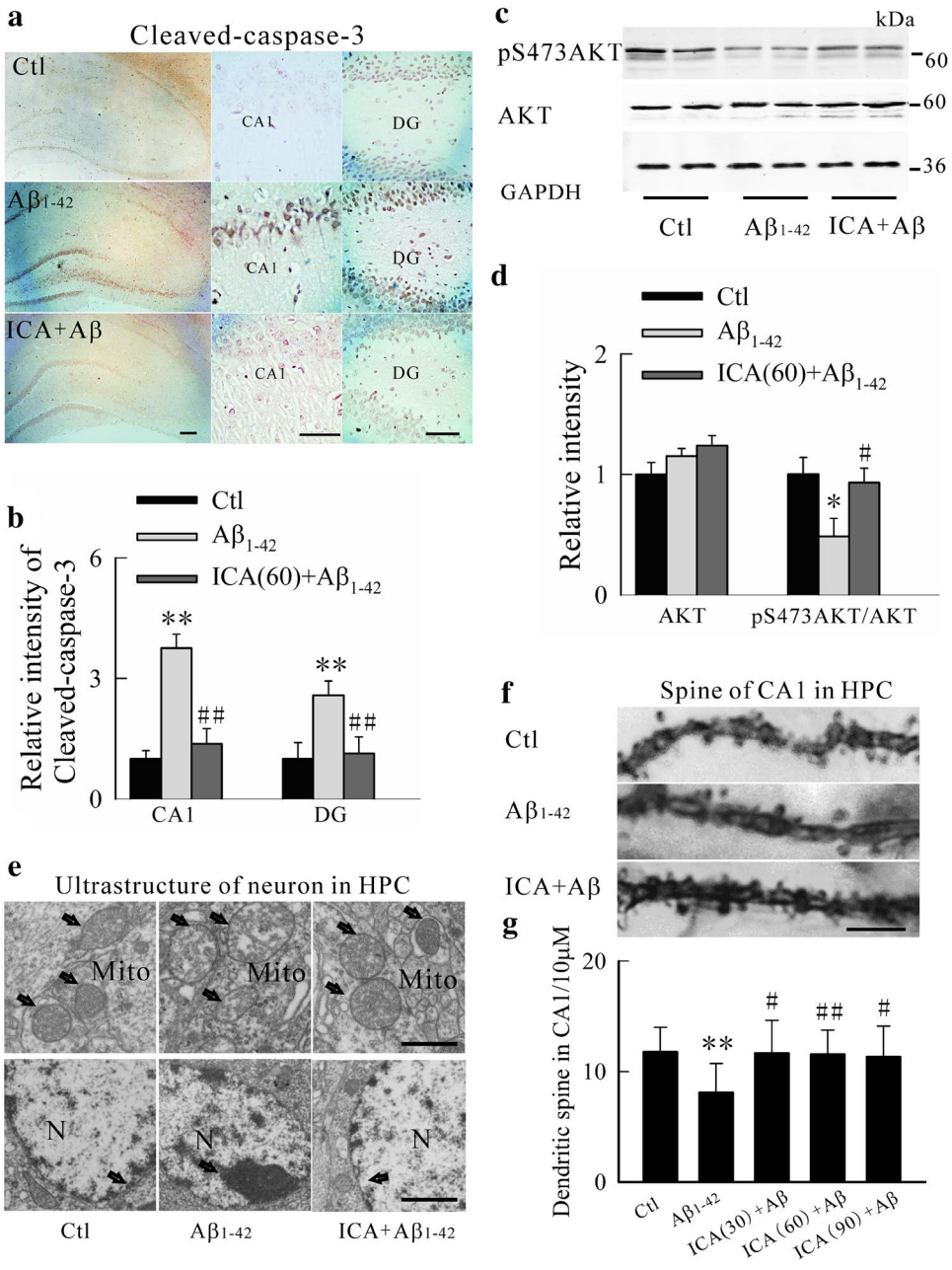

Fig. 5 ICA reduces Cleaved-caspase-3 expression and rescues ultrastructure of mitochondrias and nuclei in the hippocampus of $A\beta_{1–42}$ icv injected rats. **a**, **b** Immunohistochemistry and quantification of Cleaved-caspase-3 in CA1 and DG of hippocampus. Scale bars: 10 μμm; **c** PS473Akt and total AKT were tested by Western blotting; **d** Quantitative analysis for proportions of AKT/GAPDH and pS473AKT/AKT; **e** Control rats had normal mitochondrias with two bounding membranes enriched in regions of active synapses and nuclei possess clear membranes. $A\beta_{1–42}$ icv injected rats had damage mitochondrias reflected by the degree of the swelling in dystrophic neurites (arrows) and nuclei had unclear nuclear membranes and abundant nuclease chromatin agglutinates, however, ICA ameliorated the organelles structure. Scale bars: 1 μm; **f**, **g** Quantification for dendritic spines intensity of apical segment of CA1. Scale bars: 10 μm. Data were expressed as mean ± SD. Mito, mitochondria; *N* nucleus; $^{*}p<0.05$; $^{**}p<0.01$ vs Ctl (control group); $^{\#}p<0.05$; $^{\#\#}p<0.01$ vs $A\beta_{1–42}$ ($A\beta_{1–42}$ icv-injected group)

(arrows) and nuclei with unclear nuclear membranes and abundant nucleas chromatin agglutinates, suggesting that $A\beta_{1–42}$ cause neuronal apoptosis in vivo. ICA obviously ameliorated $A\beta_{1–42}$-induced severely disrupted organelles structures in hippocampus (Fig. 5e). Aβ accumulation was associated with aberrant synaptic structure in the hippocampus of APP transgenic mice [55]. A significant increase of spine density in hippocampal CA1 region was observed in ICA administration groups, which was decreased in $A\beta_{1–42}$ rats detected by Golgi staining (Fig. 5f, g).

It was well known that glia cells can produce inflammatory cytokines as well as generate Aβ when they are activated [56]. Glial fibrillary acidic protein (GFAP)-positive cell numbers was increased by 30% 5 weeks after $A\beta_{1–42}$ injection in the hippocampus compared to control rats, whereas ICA revealed a decrease in the expression (Fig. 6a, b).

Prevention of ICA Improves $A\beta_{1–42}$-induced Cognitive Deficits and Autophagic Dysfunction

Finally, we compared the effects of prevention and treatment ICA (60 mg/day) on spatial memory retention in this non-transgenic AD model animals. The timeline of the prevention and treatment experiments is described as Fig. 7a. For prevention and cure studies, ICA was provided before or

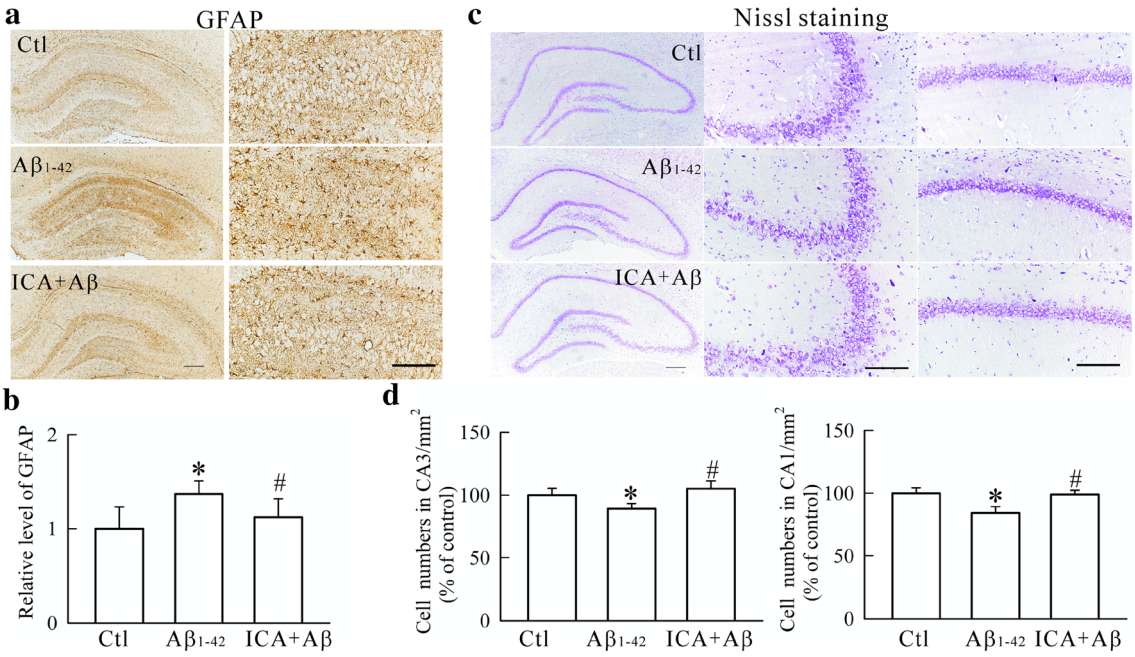

Fig. 6 ICA reduces astroglial reaction and rescues cell loss in hippocampus of $A\beta_{1–42}$ icv injected rats. **a**, **b** Immunohistochemistry and quantification of GFAP of hippocampus; **c**, **d** representative microphotographs of Nissl staining in hippocampus CA1 and CA3 subfields; Scale bars: 10 μm. Data were expressed as mean ± SD. $^{*}p < 0.05$ vs Ctl (control group); $^{\#}p < 0.05$ vs $A\beta_{1–42}$ ($A\beta_{1–42}$ icv-injected group)

after $A\beta_{1–42}$ injection for 4 weeks respectively. After 5 days of MWM learning trials, the mean escape latencies were significant shortened and the numbers of target quadrant crossings were increased in prevention and treatment of ICA in probe test (Fig. 7b, c). The levels of LC3-II/LC3-I and Beclin1 were lower in both the prevention and treatment groups than that in AD model group (Fig. 7e, f). Hippocampal Cathepsin D enzymatic activity assays also showed a significant decline in both the prevention and treatment groups compared with $A\beta_{1–42}$ injected group (Fig. 7d). Prevention and treatment of ICA increase $A\beta_{1–42}$-induced ratios of p-p70S6K/p70S6K (Fig. 7g, h). Electron micrographs of the CA1 hippocampal area showed that oral ICA prevention prominently attenuated Aβ-induced abundant enlarged mitochondrias and nucleas chromatin agglutinates (Fig. 7i). These results suggested that both prevention and treatment of ICA improves $A\beta_{1–42}$-induced cognitive deficits, pathological changes and autophagic dysfunction.

Discussion

In the present study, we have found that ICA effectively reversed $A\beta_{1–42}$-induced spatial memory deficits and pathological changes in a Non-transgenic Alzheimer's animal model. Oral supplement of ICA after $A\beta_{1–42}$ icv injection suppressed Aβ, reversed Aβ-induced autophagic process activation, enhanced p70S6K and preserved mitochondrias and nucleas damage, and most importantly, attenuated the cognitive impairments.

We use icv infusion of $A\beta_{1–42}$ human peptide in rats rather than AD transgenic mice to simulate the specific role of Aβ peptides per se in development of AD pathology, since familial genetic mutations are responsible for only a small portion of AD cases [57]. One of our findings is that a single icv injection of $A\beta_{1–42}$ provoked behavioral, biochemical and morphological alterations 5 weeks after injection, suggesting Aβ oligomers are highly neurotoxic. In this work, long-lasting effects of Aβ oligomers injection modified APP processing. At present, the underlying mechanism by which Aβ treatment can induce expression or processing of APP remains unclear. Some earlier reports have shown that Aβ peptide can bind to an Aβ-interacting domain in a sequence-specific manner in the promoter region of APP and BACE1. Thus, it is possible that Aβ peptide may act as transcription factor or cofactor in its own right to regulate the expression of APP and BACE1 [58–60]. Moreover, astrocytes following exposure to Aβ enhance levels of APP leading to increased production/secretion of Aβ-related peptides, contributing directly to the progression of AD pathology [56, 61]. Agreement with earlier studies, we discovered that Aβ injection produced a sustained increase of glia cells activity, maybe related to the rise of Aβ production. Besides, strong evidence indicates that autophagy is an active pathway for

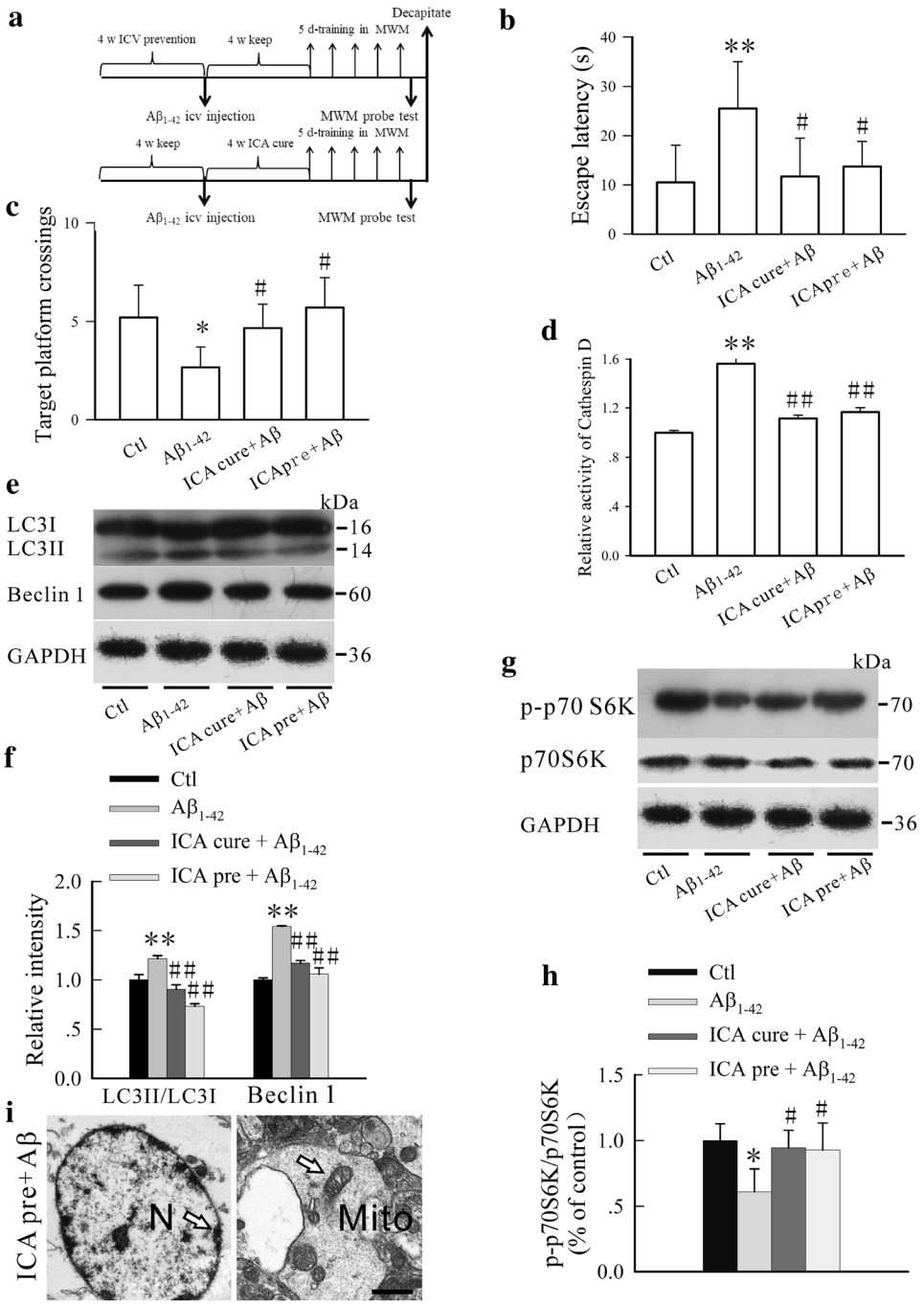

Fig. 7 Both prevention and treatment of ICA improves cognitive deficits and reverses of autophagy dysfunction in $A\beta_{1–42}$ injected rats. **a** A schematic diagram for the prevention and treatment of the rats. Behavioral tests and quantitative analyses in the comparison between prevention and treatment of ICA experiment. The escape latencies (**b**) and numbers of target platform crossings (**c**) were recorded in probe test (n = 10 rats each group); **d** enzymatic activities of Cathepsin D in brains; **e** western blotting and **f** quantitative analysis for LC3 and Beclin 1 from the hippocampus; **g** p-p70S6K and total p70S6K were detected by Western blotting; **h** quantitative analysis of p-p70S6K/p70S6K; **i** electron micrographs of the CA1 hippocampal area. ICA prevention ameliorated Aβ-induced abundant enlarged mitochondrias and nucleas chromatin agglutinates. Scale bars: 1 μm. Data were expressed as mean ± SD. Mito, mitochondria; N, nucleus; $^{*}p < 0.05$; $^{**}p < 0.01$ vs Ctl (control group); $^{\#}p < 0.05$; $^{\#\#}p < 0.01$ vs $A\beta_{1–42}$ ($A\beta_{1–42}$ icv-injected group)

APP processing and Aβ production and degradation in pathological conditions [23]. These findings may explain human $A\beta_{1–42}$ infusion led to rise of APP expression, endogenous rat $A\beta_{42}$ levels and hippocampal 6E10-positive cells in present study. ICA treatments decreased endogenous rat $A\beta_{42}$ after exogenously Aβ administration, implying that the extracellular Aβ-degrading enzyme activity had increased or the intracellular uptake of Aβ had increased. The detailed mechanisms of the phenomena should be explored, for instance, neprilysin (NEP), insulin-degrading enzyme (IDE), matrix metallopeptidases (MMPs) and receptor for advanced glycation end products (RAGE) pathway would be detected in our future research.

As examined by Western blotting, it could be suggested that the function of ICA (90 mg/kg) is to suppress the increase in expression level of 22C11 induced by Aβ. We suspect that ICA (90 mg/kg) may inhibit APP protein transcription or increase APP protein degradation. APP mRNA and ubiquitination level of APP need to be detected in further experiments. Unexpected, compared with control group,

ICA (90 mg/kg) alone enhanced the ratios of LC3-II/LC3-I with no changes of Beclin1 and Cat D. We propose that ICA at dose of 90 mg/kg is through its dual functions in regulating autophagy. Under normal conditions, ICA (90 mg/kg) increased autophagosome formation, while, it restrained overactivation of autophagy trigged by Aβ.

Deficient autophagy is implicated in the development of AD progression, manifesting that induction and maturation of autophagosomes are impaired. The autophagosomes tend to accumulate markedly in dystrophic neurites before Aβ deposition at young ages of APP/PS1 transgenic mice, indicating that induction of autophagy is an early response in AD. To date, many studied about $A\beta_{1-42}$ on autophagic pathway on different conditions include (i) that A 24 h incubation with Aβ in SH-SY5Y cells results that have damaged lysosomes and accumulate autophagic vacuoles [62]; (ii) that Aβ induced astrocyte dysfunction in autophagic activation and up-regulated inflammatory secretion [63]; (iii) that autophagy was suppressed after $A\beta_{42}$ exposure in the cultured hippocampal neurons [64]; and (iv) $A\beta_{1-42}$ induced strong autophagy response with increase of the autophagosome formation and the conversion of EGFP-LC3-I to EGFP-LC3-II after 4 h incubation in SH-SY5Y/pEGFP-LC3 [49]. Our data indicate that that $A\beta_{1-42}$ produced a long-term increase of autophagic process even 5 weeks after the injection, reflecting increase of LC3-II, Cathepsin D and Beclin 1 protein levels and Cathepsin D enzymatic activity in vivo. Report from JCI showed that Beclin 1 was strongly reduced in the brains of AD patients [29], while, it was increased in our AD model rats. This discrepancy may be due to different AD model animals we used. Here, we also found that P62 did not manifest any differences among these groups. If autophagic flux is unobstructed, the increase of LC3-II turnover is accompanied with decrease of P62 protein. These results suggested that autophagic flux is blocked in $A\beta_{1-42}$ icv injected rats.

Our work demonstrated that ICA inhibited $A\beta_{1-42}$-induced autophagic process activation, which partially consistent with the recent study [65]. Conversely, some articles claim that the upregulation of autophagy is a promising therapeutic target, promoting the clearance of aggregate-prone proteins. For instance, activation of autophagy in mice transgenic for human mutant P301S tau decreased the number of tau inclusions and increased nerve cell survival in cerebral cortex and brain stem [66]; application of the autophagy enhancer rapamycin may alleviate the cognitive impairment and Aβ neuropathology in animal model of AD [67]; induction of the autophagy pathway by enhancing Beclin1 activity reduces intracellular and extracellular Aβ in APP transgenic mice [29]. Although activation of autophagy is known to play a preventive measure to combat onset of some neurodegenerative diseases including early stages of AD, upregulation of autophagic process may backfire if applied to later stages of AD, in which toxic oligomeric Aβ is progressively released. These observations raise the question of whether inducing of autophage is beneficial or detrimental to AD depends on the context. Because activation or inhibition of autophagy alone maybe have an unintended side effect on AD treatment, therefore, keeping autophage flux homeostasis can be a strategy for prevention and treatment of AD.

It was reported that ROS play an essential function in the induction of the type III PI3 kinase and autophagy in response to Aβ [68]. Alternatively, ICA can be metabolized into icariside II by intestinal flora after oral administration. Icariside II is considered to be a novel phosphodiesterase 5 (PDE5) inhibitor, reducing ROS levels and restoring mitochondrial function [69]. Especially, PDE5 is upregulated in temporal cortex of AD patients [70]. Combined with our results, we speculated that ICA serve as oxidative metabolites scavenger and against Aβ-triggered oxidative stress, raising the possibility that inhibiting $A\beta_{1-42}$-induced oxidative stress and autophagic process.

Besides its ability to keeping autophage flux, ICA may be involved in anti-apoptotic effects presenting decline of caspase-3 activity and improvement of hippocampal ultrastructure. First, we examined that ICA efficiently inhibited Cleaved-caspase-3 and increased the activity of AKT reflected by the increase of pS473AKT/AKT. Furthermore, ICA significantly attenuated Aβ-induced defective mitochondrias, abundant nucleas chromatin agglutinates of nuclei and the number of dendritic spines in hippocampus. Taken together, our results indicate that ICA can reduce the amount of Aβ aggregates, maintain homeostasis of autophagic systems and even improve cognitive deficits in $A\beta_{1-42}$ icv injected rats and traditional Chinese herb maybe beneficial to AD.

Acknowledgements This work was supported by National Natural Science Foundation of China (81303252, 81573865), Hubei Provincial Natural Science Foundation of China (2017CFB733) and China Postdoctoral Science Special Foundation (2016T90685).

Compliance with Ethical Standards

Conflict of interest The authors declare that they have no potential conflicts of interest to disclose.

References

1. Abraham CR, Selkoe DJ, Potter H (1988) Immunochemical identification of the serine protease inhibitor alpha 1-antichymotrypsin in the brain amyloid deposits of Alzheimer's disease. Cell 52(4):487–501. https://doi.org/10.1016/0092-8674(88)90462-x
2. Selkoe DJ (2001) Alzheimer's disease: genes, proteins, and therapy. Physiol Rev 81(2):741–765. https://doi.org/10.1152/physrev.2001.81.2.741

3. Price DL, Tanzi RE, Borchelt DR, Sisodia SS (1998) Alzheimer's disease: genetic studies and transgenic models. Annu Rev Genet 32:461–493. https://doi.org/10.1146/annurev.genet.32.1.461
4. Neve RL, McPhie DL, Chen Y (2000) Alzheimer's disease: a dysfunction of the amyloid precursor protein. Brain Res 886(1–2):54–66. https://doi.org/10.1016/s0006-8993(00)02869-9
5. Wilcock GK, Esiri MM (1982) Plaques, tangles and dementia. A quantitative study. J Neurol Sci 56(2–3):43–356. https://doi.org/10.1016/0022-510x(82)90155-1
6. Arriagada PV, Growdon JH, Hedley-Whyte ET, Hugman B (1992) Neurofibrillary tangles but not senile plaques parallel duration and severity of Alzheimer's disease. Neurology 42(3 Pt 1):631–639. https://doi.org/10.1212/wnl.42.3.631
7. Hsia AY, Masliah E, McConlogue L, Yu GQ, Tatsuno G, Hu K, Kholodenko D, Malenka RC, Nicoll RA, Mucke L (1996) Plaque-independent disruption of neural circuits in Alzheimer's disease mouse models. Proc Natl Acad Sci USA 96(6):3228–3233. https://doi.org/10.1073/pnas.96.6.3228
8. Guillozet AL, Weintraub S, Mash DC, Mesulam MM (2003) Neurofibrillary tangles, amyloid, and memory in aging and mild cognitive impairment. Arch Neurol 60(5):729–736. https://doi.org/10.1001/archneur.60.5.729
9. Koistinaho M, Ort M, Cimadevilla JM, Vondrous R, Cordell B, Koistinaho J, Bures J, Higgins LS (2001) Specific spatial learning deficits become severe with age in beta -amyloid precursor protein transgenic mice that harbor diffuse beta -amyloid deposits but do not form plaques. Proc Natl Acad Sci USA 98(25):14675–14680. https://doi.org/10.1073/pnas.261562998
10. LaFerla FM, Green KN, Oddo S (2007) Intracellular amyloid-beta in Alzheimer's disease. Nat Rev Neurosci 8(7):499–509. https://doi.org/10.1038/nrn2168
11. Hughes B, Herron CE (2019) Cannabidiol reverses deficits in hippocampal LTP in a model of Alzheimer's disease. Neurochem Res 44(3):703–713. https://doi.org/10.1007/s11064-018-2513-z
12. Stéphan A, Laroche S, Davis S (2001) Generation of aggregated beta-amyloid in the rat hippocampus impairs synaptic transmission and plasticity and causes memory deficits. J Neurosci 21(15):5703–5714. https://doi.org/10.1523/jneurosci.21-15-05703.2001
13. Lee SJ, Liyanage U, Bickel PE, Xia W, Lansbury PT Jr, Kosik KS (1998) A detergent-insoluble membrane compartment contains A beta in vivo. Nat Med 4(6):730–734. https://doi.org/10.1038/nm0698-730
14. Dahlgren KN, Manelli AM, Stine WB Jr, Baker LK, Krafft GA, LaDu MJ (2002) Oligomeric and fibrillar species of amyloid-beta peptides differentially affect neuronal viability. J Biol Chem 277(35):32046–32053. https://doi.org/10.1074/jbc.m201750200
15. Lambert MP, Barlow AK, Chromy BA, Edwards C, Freed R, Liosatos M, Morgan TE, Rozovsky I, Trommer B, Viola KL, Wals P, Zhang C, Finch CE, Krafft GA, Klein WL (1998) Diffusible, nonfibrillar ligands derived from Abeta$_{1–42}$ are potent central nervous system neurotoxins. Proc Natl Acad Sci USA 95(11):6448–6453. https://doi.org/10.1073/pnas.95.11.6448
16. Malm T, Ort M, Tähtivaara L, Jukarainen N, Goldsteins G, Puoliväli J, Nurmi A, Pussinen R, Ahtoniemi T, Miettinen TK, Kanninen K, Leskinen S, Vartiainen N, Yrjänheikki J, Laatikainen R, Harris-White ME, Koistinaho M, Frautschy SA, Bures J, Koistinaho J (2006) beta-Amyloid infusion results in delayed and age-dependent learning deficits without role of inflammation or beta-amyloid deposits. Proc Natl Acad Sci USA 103(23):8852–8857. https://doi.org/10.1073/pnas.0602896103
17. Nabeshima T, Nitta A (1994) Memory impairment and neuronal dysfunction induced by beta-amyloid protein in rats. Tohoku J Exp Med 174(3):241–249. https://doi.org/10.1620/tjem.174.241
18. Goedert M, Clavaguera F, Tolnay M (2010) The propagation of prion-like protein inclusions in neurodegenerative diseases. Trends Neurosci 33(7):317–325. https://doi.org/10.1016/j.tins.2010.04.003
19. Goldberg AL (2003) Protein degradation and protection against misfolded or damaged proteins. Nature 426(6968):895–899. https://doi.org/10.1038/nature02263
20. Klionsky DJ, Emr SD (2000) Autophagy as a regulated pathway of cellular degradation. Science 290(5497):1717–1721. https://doi.org/10.1126/science.290.5497.1717
21. Levine B (2005) Eating oneself and uninvited guests: autophagy-related pathways in cellular defense. Cell 120(2):159–162. https://doi.org/10.1016/j.cell.2005.01.005
22. Eskelinen EL (2005) Maturation of autophagic vacuoles in mammalian cells. Autophagy 1(1):1–10. https://doi.org/10.4161/auto.1.1.1270
23. Nixon RA (2007) Autophagy, amyloidogenesis and Alzheimer disease. J Cell Sci 120(Pt 23):4081–4091. https://doi.org/10.1242/jcs.019265
24. Yu WH, Kumar A, Peterhoff C, Shapiro Kulnane L, Uchiyama Y, Lamb BT, Cuervo AM, Nixon RA (2004) Autophagic vacuoles are enriched in amyloid precursor protein-secretase activities: implications for β-amyloid peptide overproduction and localization in Alzheimer's disease. Int J Biochem Cell Biol 36(12):2531–2540. https://doi.org/10.1016/j.biocel.2004.05.010
25. Ułamek-Kozioł M, Furmaga-Jabłońska W, Januszewski S, Brzozowska J, Sciślewska M, Jabłoński M, Pluta R (2013) Neuronal autophagy: self-eating or self-cannibalism in Alzheimer's disease. Neurochem Res 38(9):1769–1773. https://doi.org/10.1007/s11064-013-1082-4
26. Hara T, Nakamura K, Matsui M, Yamamoto A, Nakahara Y, Suzuki-Migishima R, Yokoyama M, Mishima K, Saito I, Okano H, Mizushima N (2006) Suppression of basal autophagy in neural cells causes neurodegenerative disease in mice. Nature 441(7095):885–889. https://doi.org/10.1038/nature04724
27. Komatsu M, Waguri S, Chiba T, Murata S, Iwata J, Tanida I, Ueno T, Koike M, Uchiyama Y, Kominami E, Tanaka K (2006) Loss of autophagy in the central nervous system causes neurodegeneration in mice. Nature 441(7095):880–884. https://doi.org/10.1038/nature04723
28. Yang DS, Stavrides P, Mohan PS, Kaushik S, Kumar A, Ohno M, Schmidt SD, Wesson D, Bandyopadhyay U, Jiang Y, Pawlik M, Peterhoff CM, Yang AJ, Wilson DA, St George-Hyslop P, Westaway D, Mathews PM, Levy E, Cuervo AM, Nixon RA (2011) Reversal of autophagy dysfunction in the TgCRND8 mouse model of Alzheimer's disease ameliorates amyloid pathologies and memory deficits. Brain 134(Pt 1):258–277. https://doi.org/10.1093/brain/awq341
29. Pickford F, Masliah E, Britschgi M, Lucin K, Narasimhan R, Jaeger PA, Small S, Spencer B, Rockenstein E, Levine B, Wyss-Coray T (2008) The autophagy-related protein beclin 1 shows reduced expression in early Alzheimer disease and regulates amyloid beta accumulation in mice. J Clin Invest 118(6):2190–2199. https://doi.org/10.1172/JCI33585
30. Ma HP, Ming LG, Ge BF, Zhai YK, Song P, Xian CJ, Chen KM (2011) Icariin is more potent than genistein in promoting osteoblast differentiation and mineralization in vitro. J Cell Biochem 112(3):916–923. https://doi.org/10.1002/jcb.23007
31. Wang Z, Zhang X, Wang H, Qi L, Lou Y (2007) Neuroprotective effects of icaritin against beta amyloid-induced neurotoxicity in primary cultured rat neuronal cells via estrogen-dependent pathway. Neuroscience 145(3):911–922. https://doi.org/10.1016/j.neuroscience.2006.12.059
32. Xu CQ, Liu BJ, Wu JF, Xu YC, Duan XH, Cao YX, Dong JC (2010) Icariin attenuates LPS-induced acute inflammatory responses: involvement of PI3 K/Akt and NF-κB signaling pathway. Eur J Pharmacol 642(1–3):146–153. https://doi.org/10.1016/j.ejphar.2010.05.012

33. Zhou J, Wu J, Chen X, Fortenbery N, Eksioglu E, Kodumudi KN, Pk EB, Dong J, Djeu JY, Wei S (2011) Icariin and its derivative, ICT, exert anti- inflammatory, anti-tumor effects, and modulate myeloid derived suppressive cells (MDSCs) functions. Int Immunopharmacol 11(7):887–895. https://doi.org/10.1016/j.intimp.2011.01.007
34. Wu B, Chen Y, Huang J, Ning Y, Bian Q, Shan Y, Cai W, Zhang X, Shen Z (2012) Icariin improves cognitive deficits and activates quiescent neural stem cells in aging rats. J Ethnopharmacol 142(3):746–753. https://doi.org/10.1016/j.jep.2012.05.056
35. Nie J, Luo Y, Huang XN, Gong QH, Wu Q, Shi JS (2010) Icariin inhibits β-amyloid peptide segment 25-35 induced expression of beta-secretase in rat hippocampus. Eur J Pharmacol 626(2–3):213–218. https://doi.org/10.1016/j.ejphar.2009.09.039
36. He XL, Zhou WQ, Bi MG, Du GH (2010) Neuroprotective effects of icariin on memory impairment and neurochemical deficits in senescence-accelerated mouse prone 8 (SAMP8) mice. Brain Res 1334:73–83. https://doi.org/10.1016/j.brainres.2010.03.084
37. Urano T, Tohda C (2010) Icariin improves memory impairment in Alzheimer's disease model mice (5xFAD) and attenuates amyloid β-induced neurite atrophy. Phytother Res 24(11):1658–1663. https://doi.org/10.1002/ptr.3183
38. Zeng KW, Ko H, Yang HO, Wang XM (2010) Icariin attenuates β-amyloid-induced neurotoxicity by inhibition of tau protein hyperphosphorylation in PC12 cells. Neuropharmacology 59(6):542–550. https://doi.org/10.1016/j.neuropharm.2010.07.020
39. Sheng C, Xu P, Zhou K, Deng D, Zhang C, Wang Z (2017) Icariin attenuates synaptic and cognitive deficits in an $A\beta_{1-42}$-induced rat model of Alzheimer's disease. Biomed Res Int 2017:7464872. https://doi.org/10.1155/2017/7464872
40. Zhang L, Shen C, Chu J, Zhang R, Li Y, Li L (2014) Icariin decreases the expression of APP and BACE-1 and reduces the β-amyloid burden in an APP transgenic mouse model of Alzheimer's disease. Int J Biol Sci 10(2):181–191. https://doi.org/10.7150/ijbs.6232
41. Wang GQ, Li DD, Huang C, Lu DS, Zhang C, Zhou SY, Liu J, Zhang F (2018) Icariin reduces dopaminergic neuronal loss and microglia-mediated inflammation in vivo and in vitro. Front Mol Neurosci 10:441. https://doi.org/10.3389/fnmol.2017.00441
42. Zhu L, Li D, Chen C, Wang G, Shi J, Zhang F (2019) Activation of Nrf2 signaling by Icariin protects against 6-OHDA-induced neurotoxicity. Biotechnol Appl Biochem 10000:10000. https://doi.org/10.3389/fnmol.2017.00441
43. Zeng J, Jiang X, Hu XF, Ma RH, Chai GS, Sun DS, Xu ZP, Li L, Bao J, Feng Q, Hu Y, Chu J, Chai DM, Hong XY, Wang JZ, Liu GP (2016) Spatial training promotes short-term survival and neuron-like differentiation of newborn cells in $A\beta_{1-42}$-injected rats. Neurobiol Aging 45:64–75. https://doi.org/10.1016/j.neurobiolaging.2016.05.005
44. Liu SJ, Zhang AH, Li HL, Wang Q, Deng HM, Netzer WJ, Xu H, Wang JZ (2003) Overactivation of glycogen synthase kinase-3 by inhibition of phosphoinositol-3 kinase and protein kinase C leads to hyperphosphorylation of tau and impairment of spatial memory. J Neurochem 87(6):1333–1344. https://doi.org/10.1046/j.1471-4159.2003.02070.x
45. Jiang X, Tian Q, Wang Y, Zhou XW, Xie JZ, Wang JZ, Zhu LQ (2011) Acetyl-L-carnitine ameliorates spatial memory deficits induced by inhibition of phosphoinositol-3 kinase and protein kinase C. J Neurochem 118(5):864–878. https://doi.org/10.1111/j.1471-4159.2011.07355.x
46. Xu S, Yu J, Zhan J, Yang L, Guo L, Xu Y (2017) Pharmacokinetics, tissue distribution, and metabolism study of icariin in rat. Biomed Res Int 2017:4684962. https://doi.org/10.1155/2017/4684962
47. Jiang X, Jia LW, Li XH, Cheng XS, Xie JZ, Ma ZW, Xu WJ, Liu Y, Yao Y, Du LL, Zhou XW (2013) Capsaicin ameliorates stress-induced Alzheimer's disease-like pathological and cognitive impairments in rats. J Alzheimers Dis 35(1):91–105. https://doi.org/10.3233/JAD-121837
48. Tanida I, Ueno T, Kominami E (2008) LC3 and autophagy. Methods Mol Biol 445:77–88. https://doi.org/10.1007/978-1-59745-157-4_4
49. Hung SY, Huang WP, Liou HC, Fu WM (2009) Autophagy protects neuron from Abeta-induced cytotoxicity. Autophagy 5(4):502–510. https://doi.org/10.4161/auto.5.4.8096
50. Liang XH, Jackson S, Seaman M, Brown K, Kempkes B, Hibshoosh H, Levine B (1999) Induction of autophagy and inhibition of tumorigenesis by beclin 1. Nature 402(6762):672–676. https://doi.org/10.1038/45257
51. Guglielmotto M, Monteleone D, Piras A, Valsecchi V, Tropiano M, Ariano S, Fornaro M, Vercelli A, Puyal J, Arancio O, Tabaton M, Tamagno E (2014) $A\beta_{1-42}$ monomers or oligomers have different effects on autophagy and apoptosis. Autophagy 10(10):1827–1843. https://doi.org/10.4161/auto.30001
52. Hong WK, Han EH, Kim DG, Ahn JY, Park JS, Han BG (2007) Amyloid-beta-peptide reduces the expression level of mitochondrial cytochrome oxidase subunits. Neurochem Res 32(9):1483–1488. https://doi.org/10.1007/s11064-007-9336-7
53. Chong YH, Shin YJ, Lee EO, Kayed R, Glabe CG, Tenner AJ (2006) ERK1/2 activation mediates Abeta oligomer-induced neurotoxicity via caspase-3 activation and tau cleavage in rat organotypic hippocampal slice cultures. J Biol Chem 281(29):20315–20325. https://doi.org/10.1074/jbc.M601016200
54. Yin G, Li LY, Qu M, Luo HB, Wang JZ, Zhou XW (2011) Upregulation of AKT attenuates amyloid-β-induced cell apoptosis. J Alzheimers Dis 25(2):337–345. https://doi.org/10.3233/JAD-2011-110104
55. Jacobsen JS, Wu CC, Redwine JM, Comery TA, Arias R, Bowlby M, Martone R, Morrison JH, Pangalos MN, Reinhart PH, Bloom FE (2006) Early-onset behavioral and synaptic deficits in a mouse model of Alzheimer's disease. Proc Natl Acad Sci USA 103(13):5161–5166. https://doi.org/10.1073/pnas.0600948103
56. Moreno-Flores MT, Salinero O, Wandosell F (1998) BetaA amyloid peptide (25-35) induced APP expression in cultured astrocytes. J Neurosci Res 52(6):661–671. https://doi.org/10.1002/(SICI)1097-4547(19980615)52:6%3c661:AID-JNR5%3e3.0.CO;2-6
57. Hardy J, Duff K, Hardy KG, Perez-Tur J, Hutton M (1998) Genetic dissection of Alzheimer's disease and related dementias: amyloid and its relationship to tau. Nat Neurosci 1(5):355–358. https://doi.org/10.1038/1565
58. Piccini A, Borghi R, Guglielmotto M, Tamagno E, Cirmena G, Garuti A, Pollero V, Cammarata S, Fornaro M, Messa M, Colombo L, Salmona M, Perry G, Tabaton M (2012) β-amyloid 1-42 induces physiological transcriptional regulation of BACE1. J Neurochem 122(5):1023–1031. https://doi.org/10.1111/j.1471-4159.2012.07834.x
59. Maloney B, Lahiri DK (2011) The Alzheimer's amyloid β-peptide (Aβ) binds a specific DNA Aβ-interacting domain (AβID) in the APP, BACE1, and APOE promoters in a sequence-specific manner: characterizing a new regulatory motif. Gene 488(1–2):1–12. https://doi.org/10.1016/j.gene.2011.06.004
60. Bailey JA, Maloney B, Ge YW, Lahiri DK (2011) Functional activity of the novel Alzheimer's amyloid β-peptide interacting domain (AβID) in the APP and BACE1 promoter sequences and implications in activating apoptotic genes and in amyloidogenesis. Gene 488(1–2):13–22. https://doi.org/10.1016/j.gene.2011.06.017
61. Ourdev D, Foroutanpay BV, Wang Y, Kar S (2015) The effect of $A\beta_{1-42}$ oligomers on APP processing and $A\beta_{1-40}$ generation in cultured U-373 astrocytes. Neurodegener Dis 15(6):361–368. https://doi.org/10.1159/000438923

62. Soura V, Stewart-Parker M, Williams TL, Ratnayaka A, Atherton J, Gorringe K, Tuffin J, Darwent E, Rambaran R, Klein W, Lacor P, Staras K, Thorpe J, Serpell LC (2012) Visualization of co-localization in Aβ42-administered neuroblastoma cells reveals lysosome damage and autophagosome accumulation related to cell death. Biochem J 441(2):579–590. https://doi.org/10.1042/BJ20110749
63. Hong Y, Liu Y, Zhang G, Wu H, Hou Y (2018) Progesterone suppresses Aβ42-induced neuroinflammation by enhancing autophagy in astrocytes. Int Immunopharmacol 54:336–343. https://doi.org/10.1016/j.intimp.2017.11.044
64. Yin Y, Zhao Y, Han S, Zhang N, Chen H, Wang X (2017) Autophagy-ERK1/2-involved disinhibition of hippocampal neurons contributes to the pre-synaptic toxicity induced by Aβ42 exposure. J Alzheimers Dis 59(3):851–869. https://doi.org/10.3233/JAD-170246
65. Chen FJ, Liu B, Wu Q, Liu J, Xu YY, Zhou SY, Shi JS (2019) Icariin delays brain aging in Senescence-Accelerated Mouse Prone 8 (SAMP8) model via inhibiting autophagy. J Pharmacol Exp Ther 369(1):121–128. https://doi.org/10.1124/jpet.118.253310
66. Tramutola A, Lanzillotta C, Di Domenico F (2017) Targeting mTOR to reduce Alzheimer-related cognitive decline: from current hits to future therapies. Expert Rev Neurother 17(1):33–45. https://doi.org/10.1080/14737175.2017.1244482
67. Schaeffer V, Lavenir I, Ozcelik S, Tolnay M, Winkler DT, Goedert M (2012) Stimulation of autophagy reduces neurodegeneration in a mouse model of human tauopathy. Brain 135(Pt 7):2169–2177. https://doi.org/10.1093/brain/aws143
68. Lipinski MM, Zheng B, Lu T, Yan Z, Py BF, Ng A, Xavier RJ, Li C, Yankner BA, Scherzer CR, Yuan J (2010) Genome-wide analysis reveals mechanisms modulating autophagy in normal brain aging and in Alzheimer's disease. Proc Natl Acad Sci USA 107(32):14164–14169. https://doi.org/10.1073/pnas.1009485107
69. Gao J, Deng Y, Yin C, Liu Y, Zhang W, Shi J, Gong Q (2017) Icariside II, a novel phosphodiesterase 5 inhibitor, protects against H_2O_2-induced PC12 cells death by inhibiting mitochondria-mediated autophagy. J Cell Mol Med 21(2):375–386. https://doi.org/10.1111/jcmm.12971
70. Teich AF, Sakurai M, Patel M, Holman C, Saeed F, Fiorito J, Arancio O (2016) PDE5 exists in human neurons and is a viable therapeutic target for neurologic disease. J Alzheimers Dis 52(1):295–302. https://doi.org/10.3233/JAD-151104